Foods and Raw Materials. 2026;14(2)

ISSN 2308-4057 (Print)
ISSN 2310-9599 (Online)

Research Article
Open Access

Available online at http://jfrm.ru/en
https://doi.org/10.21603/2308-4057-2026-2-684
https://elibrary.ru/SYRDUP

Experimental recirculating carbon dioxide refrigeration unit

Evgeniy N. Neverov*, Pavel S. Korotkih, Alena K. Gorelkina, Irina V. Timoshchuk

Kemerovo State University, Kemerovo, Russia

* e-mail: neverov42@mail.ru

Received 06.12.2024; Revised 13.01.2025; Accepted 03.06.2025; Published online 20.10.2025

Abstract:
Turkey farming and meat processing are fast-developing areas of the Russian food industry. However, their development requires more advanced methods of meat storage and freezing. Traditional methods of air cooling often fail to preserve the original meat texture and nutritional value. This paper introduces a new refrigeration unit with CO_2 as a refrigerant. CO_2 snow and gas come in direct contact with turkey carcasses, thus accelerating the cooling process and improving the meat quality. CO_2 recirculation makes the refrigeration unit an economical solution to environmental issues. The refrigeration unit included a conveyor system, a vacuum chamber, and a CO_2 circulation system.

The research featured grade 1 turkey carcasses of 2.7 ± 0.1 kg frozen at different temperatures (–30, –50, and –70°C) and CO_2 flux rates (0–5 m/s). The share of CO_2 in the gas mix was ≥ 50%. The temperature and heat flux density were measured using thermocouples and heat flux probes.

As the temperature dropped from –30 to –70°C, the freezing time decreased from 48 to 33 min and to 29 min when the experiment involved enforced convection. The amount of CO_2 consumed increased from 7.5 to 13.5 kg without convection and from 6.5 to 12.0 kg with enforced convection. Compared to traditional methods, CO_2 provided uniform freezing and reduced mechanical damage to the meat structure.

The newly developed refrigeration unit with recirculated CO_2 demonstrated high efficiency in freezing turkey meat while reducing CO_2 consumption and providing uniform cooling of the carcass. It demonstrated could prospects for industrial use, which opens up new opportunities for further research and freezing process optimization.

Keywords: Refrigeration, CO_2 recirculation, quick freezing, convection, turkey meat, meat processing

Funding: The research was part of a comprehensive scientific innovative program initiated by Russian Federation Government Decree No. 1144-r, May 11, 2022: Developing and implementing new technologies in the E&P of solid minerals, industrial safety, bioremediation, and product development of deep coal processing: A consistent reduction of environmental impact and hazards (Agreement No. 075-15-2022-1201, September 30, 2022).

Please cite this article in press as: Neverov EN, Korotkih PS, Gorelkina AK, Timoshchuk IV. Experimental recirculating carbon dioxide refrigeration unit. Foods and Raw Materials. 2026;15(2):377–385. https://doi.org/10.21603/2308-4057-2026-2-684

INTRODUCTION

Turkey meat production is a poultry market sector with the most value-enhancing investments and a great growth potential. As the global population and urbanization continue to grow, so does consumers' awareness of turkey meat as a healthier option than other, more traditional meats. The growing demand triggers technical advancements in processing, packaging, distribution, shelf life, and availability of turkey meat.

Today, turkey farming is concentrated in North America and Europe, where the path of industrial development has led to advanced turkey farming infrastructure. They produce enough turkey meat to meet local demand and export the surplus [1]. Russia has recently seen an increase in the number of large-scale turkey farms while small and medium-sized businesses remain scarce. The resulting random distribution of turkey meat production across regions gives the turkey industry good development perspectives, considering that some regions lack any turkey meat farms altogether [2, 3]. New effective methods for frozen storage of turkey meat may lead to a more uniform distribution of this product across Russia's regions [4].

Turkey meat is nutritious and heart-healthy: it contains little cholesterol and fat, while being rich in protein. As the demand for turkey meat increases, consumers become more and more particular about its quality. Meat

Copyright © 2025, Neverov *et al.* This is an open access article distributed under the terms of the Creative Commons Attribution 4.0 International License (https://creativecommons.org/licenses/by/4.0/), allowing third parties to copy and redistribute the material in any medium or format and to remix, transform, and build upon the material for any purpose, even commercially, provided the original work is properly cited and states its license.

quality is a complex of sensory and biological indicators that determine its practical ability to meet nutritional requirements. As for turkey meat, its quality profile includes nutritional composition, color, texture, etc. All these qualities depend on the birds' welfare. Unlike other, more traditional meats, turkey has a significant share of flesh, which gives it excellent dietary characteristics. It is rich in vitamins B, phosphorus, iron, magnesium, potassium, and amino acids. The advantage of turkey meat is that it is basically muscle tissue with a lot of labile organic substances [5–7].

Russian industrial turkey farming is young but quick-developing. A potential capacity analysis of the Russian turkey meat market shows that the volume of domestic turkey production keeps growing in terms of slaughter weight: from 30,500 tons in 2009, it skyrocketed to 125,000 tons in 2013 and rose beyond 276,000 tons in 2017 to 418,000 tons in 2023 before peaking at 512,000 tons in 2024 [8].

Freezing preserves poultry meat for transportation or long-time storage. Low temperatures extend its shelf life by inhibiting microbial spoilage and deterioration. Meat properties that are to be preserved during storage include tenderness, water-holding capacity, color, and flavor. While improving tenderness, freezing damages other characteristics, depending on the size and distribution of ice crystals, which, in their turn, depend on the rate of freezing, temperature, and storage time. Although new technologies mitigate the negative effects of freezing, the complex nature of muscle tissue makes it difficult to predict the quality of defrosted meat.

For many decades, refrigeration of poultry meat has relied on air freezing. The temperature mode and flow patterns of the cooling medium vary depending on the shelf life, packaging, and type of product. However, free (unbound) water in muscle cells becomes crystallized during freezing, which makes mechanical damage to muscle tissue inevitable. As a result, the product loses some of its nutrients. Food science is still on the lookout for more effective and modern methods of poultry freezing [9–11].

Carbon dioxide (R744) as a refrigerant provides faster freezing compared to traditional units. Fast freezing is crucial for turkey meat with its high moisture content. It minimizes coarse crystallization, helping preserve the texture and taste while extending its shelf life [12, 13]. In addition, refrigerant R744 has low environmental burden. Yet, carbon dioxide has its disadvantages as a refrigerant, which means it requires a careful selection of the system for each particular case [14–16].

Carbon dioxide as a refrigerant has some advantages over hydrochlorofluorocarbon (HCFC). For instance, R744 has a lower compression ratio than HCFC, which increases its isentropic efficiency. The cross-sectional area of the suction pipe is proportional to the volumetric capacity. For R744, the suction line diameter is twice as small as that for R404A [17]. Table 1 shows the fitting criteria of R744 for various conditions and standards.

Systems that work on CO_2 can be divided into subcritical and transcritical ones. They have the same basic CO_2 cycle: compression – heat rejection – expansion. As a result, their thermodynamic diagrams are similar, too (Fig. 1). The main difference is in the heat rejection mode.

In a subcritical cycle, heat rejection occurs below the critical point (T_c = 31.2°C, P_c = 7.38 MPa for CO_2). In the diagram of enthalpy vs. pressure, this process

Table 1 R744 vs. alternatives: Compliance with conditions and criteria

Criterion	Compliance
Refrigeration capacity	Greater displacement
Operational conditions	Higher operating pressure and resting pressure
Refrigerant	High availability
Components	Become more available as production increases
Extra qualifications	Operators need extra qualifications
Price	Cheaper cooling agent, but higher the overall expenses
Safety	Advantages: low toxic, non-flammable Disadvantages: high pressure and difficulties associated with it

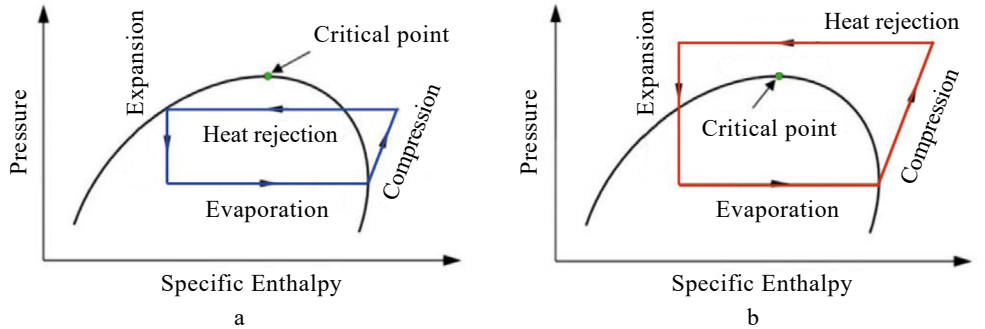


Figure 1 Working cycle of a refrigeration machine: Specific enthalpy and pressure in subcritical (a) vs. transcritical (b) systems

occurs partly within the area curbed by solid liquid (left of the critical point) and saturated vapor (right of the critical point). In the subcritical mode, heat rejection occurs as a condensation of the gaseous refrigerant at a nearly constant temperature.

In the transcritical CO_2 cycle, heat rejection occurs above the critical point, i.e., when the refrigerant is in its gaseous state. Unlike constant temperature condensation, it is a process of gas cooling [18, 19].

The systems differ in refrigeration capacity. In supercritical operation, the refrigeration capacity increases at a constant temperature as the pressure continues to grow. In the subcritical mode, the refrigeration capacity increases at lower discharge pressures.

The two systems also differ in power consumption. However, the general rule of "the lower the pressure, the lower the power consumption" is true for both systems. The change in power consumption is not proportional to the change in refrigeration capacity, which increases significantly. As a result, the amount of energy consumed by the compressor drive increases, too.

The highest performance coefficient is impossible in the supercritical mode at a minimal condensing pressure. The optimal performance coefficient (90–100 bar) depends on the evaporation conditions and the outlet temperature of the condenser. As a rule, the pressure for optimal performance is higher than for optimal efficiency [20, 21].

In transcritical systems, the pressure in the gas cooler has to be regulated to provide optimal performance while maintaining the pressure below the critical point.

R744 leaves the gas cooler at 40°C. This outlet temperature depends on the condenser size and the ambient temperature as much as the condensing temperature depends on these parameters.

Transcritical systems are designed to operate above the critical point some or all of the time. HCFC systems also go through a drop in efficiency when the ambient temperature increases. In R744 systems, the change is much greater during the transition from subcritical to transcritical cooling. Since heat rejection often occurs at ambient temperatures, some of the operating units may go subcritical in those Russian regions where the ambient temperature stays below 20–25°C.

For the transcritical mode, appropriate pressure control on the high-pressure side (condenser) is crucial as it optimizes the cooling capacity and efficiency. For example, by increasing the pressure on the high-pressure side, the machine increases its cooling capacity when operating above the critical point, which has a positive effect in the pre-cooling of poultry meat.

Like other food products, poultry has to cool down completely before packaging. Otherwise, water vapor condenses inside the package and causes molding or makes unwanted substances migrate into the product since some packaging is unsuitable for contact with warm food products. However, food enterprises see waiting for the product to cool down as a waste of time that creates practical and logistical problems. The cooling process occupies much place for many hours, which slows down the production cycles and may lead to financial losses [22, 23]. To prevent it, meat producers accelerate cooling by passing the product through a cooling tunnel with CO_2, which results in a high-quality product with a long shelf life and provides recirculation potential.

In this study, we developed and tested a refrigeration system for turkey carcasses with CO_2 as a refrigerant. The directs contact with CO_2 snow during freezing accelerated the cooling and improved the quality of meat while CO_2 recirculation minimized CO_2 losses.

STUDY OBJECTS AND METHODS

We used grade 1 turkey carcasses of 2.7 ± 0.1 kg (State Standard GOST 31473-2012).

To study the process of CO_2 freezing, we designed an experimental three-stage refrigeration unit with a heat-insulated chamber. To control the temperature, thermocouple units were installed under the turkey skin (5 ± 1 mm), inside the carcass (30 ± 5 mm), and in the inner surface of the opened turkey carcass (60 ± 10 mm) (Fig. 2). To measure the heat flux density, we placed remote heat flux probes PTP-9.9P on the surface of the carcasses.

The refrigeration unit was provided with an autonomous auxiliary low-power cooling system to prevent the pressure from increasing to emergency discharge values, when the refrigerant has to be released into the atmosphere. It also helped avoid complications caused by accidental power cut. The thermodynamic model was constructed using the Danfoss software.

Materials for the vacuum refrigeration chamber were selected based on the requirements for gas impermeability, thermal conductivity, resistance to aggressive environments, and mechanical strength. In some cases, we combined different materials. AISI 304 stainless steel served as the major material. This grade has high strength, corrosion resistance, and excellent tightness. Standard 100-millimeter-thick polyurethane foam boards provided thermal insulation.

The carcasses entered the chamber via a belt conveyor, after which the chamber was closed. Its hermetic doors were provided with PUREMIX CDM2B-40-300 double-acting pneumatic pushers, driven by a GANTA AC 260/025 air oil compressor. The chamber door was an AISI 304 steel sheet.

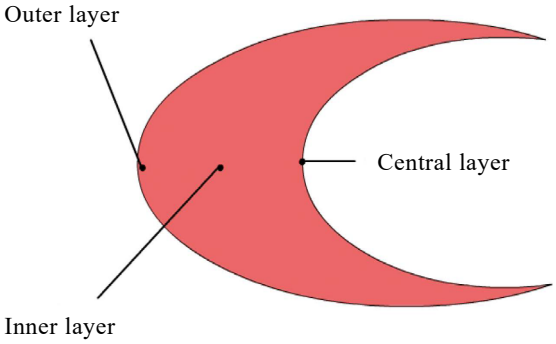


Figure 2 Temperature sensors in three layers of turkey carcass

To maintain the hermeticity along the perimeter, we used seals made of FVMQ fluorosilicone rubber. They are resistant to oils and solvents and retain their sealing ability at –80°C. The automated pneumatic system also included pneumatic stops, an air oil compressor, and compressed air preparation units. After closing the door, the limit switch gave a command to open the electromagnetic valve and turn on the Value VE-260 vacuum pump. It pumped air out of the chamber, preparing it for CO_2 intake.

The vacuuming process continued until 0.2 bar. The vacuum pump had a capacity of 170 L/min (10.2 m^3/h) to reduce the pressure in the 48-L experimental chamber to a targeted level in about 30 s.

At the next stage, liquid CO_2 was supplied to the chamber through nozzles [24]. Crystalline CO_2 settled on the product and at the bottom of the chamber. To increase the heat exchange rate, the chamber had ERA PROFIT 4 BB duct fans (100 mm across), which were responsible for artificial circulation of the gas environment.

We installed air flow velocity meters (anemometers) with an ATE-1019 remote sensor at the outlet of the fan ducts. Carbon dioxide passed through the fans, entered the side cavity of the chamber, circulated in the lower cavity, and passed through the perforated tray. The supply of CO_2 to the heat-insulated chamber stopped when the temperature in the center of the carcass reached –12°C.

Upon cooling, CO_2 snow sublimated into gas and was sucked off by the compressor through the liquid separator. The air compressor started, and the pneumatic pushers opened the doors. After the electric motor started, the conveyor started pushing the frozen product down the conveyor. The conveyor belts were strong enough and easy to clean. The latter is important because a conveyor belt consists of hinged parts that may accumulate residues of the frozen product.

Experiments on kinetics did not involve starting the conveyor and automatic doors.

RESULTS AND DISCUSSION

Figure 3 shows a diagram of a three-stage CO_2-operating subcritical-mode refrigeration unit. The first-stage compressor unit (*1*) sucked vapors out from the liquid separator (*7*) and compressed the gas to intermediate pressure 1 of 2.57 MPa. The gas entered heat exchanger I (*4*), where its temperature dropped to –15°C, after which it entered the second-stage compressor (*2*), where the gas was compressed to intermediate pressure 2 of 4.30 MPa. After that, the refrigerant moved to heat exchanger II (*4*), and then to the third-stage compressor (*3*), where the gas was compressed to the condensation pressure.

The superheated steam went to the oil separator (*5*), where oil separates from the steam. The oil then passed through oil filters to be distributed between three compressors. Hot steam entered the water-cooled condenser (*6*), where the steam condensed, and the resulting liquid entered liquid separator I (*7*). The gaseous refrigerant went back to the third-stage compressor. After that, the liquid refrigerant entered liquid separator II (*7*), where the process occurred once more. The purified refrigerant entered the linear receiver (*8*) and moved on to the chamber (*9*), with subsequent throttling and cooling. CO_2 snow sublimated into gas and was sucked out by the compressor through the liquid separator (*7*), after which the process repeated.

In the cascade heat exchanger, the evaporating third-stage refrigerant absorbed the heat removed by the condensing R744. The condensation temperature stayed below the critical point. Third-stage was a simple closed-loop chiller system controlled by the pressure in the first-stage low pressure receiver. It cooled down the load and removes heat from the condensing R744 in the first-stage cascade heat exchanger. This stage operated on R12 refrigerant. Figure 4 shows an operating cycle of the experimental three-stage refrigerator.

Table 2 summarizes the parameters of the refrigerant at the nodes.

Figure 5 shows a 3D model of the refrigerating unit (a) and the chamber in section (b).

The conveyor belt (*9.1*), driven by an electric motor (*9.2*), feeds the product to be frozen into the chamber (*9*), after which the chamber closes down with the help of double-acting pneumatic pushers (*9.3*), driven by an air oil compressor (*9.4*). After the door is closed, the vacuum pump (*9.5*) sucks air out until vacuum is reached, after which refrigerant R744 enters the chamber through

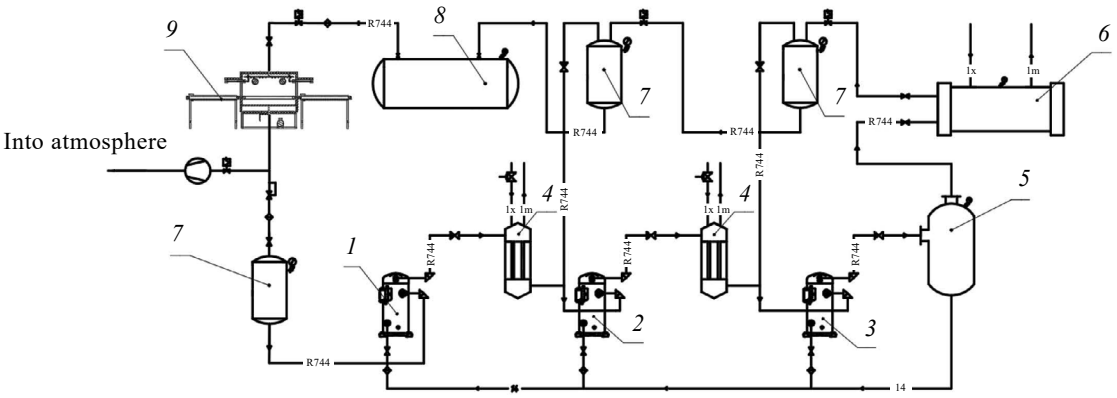


Figure 3 Three-stage CO_2-operating refrigerator

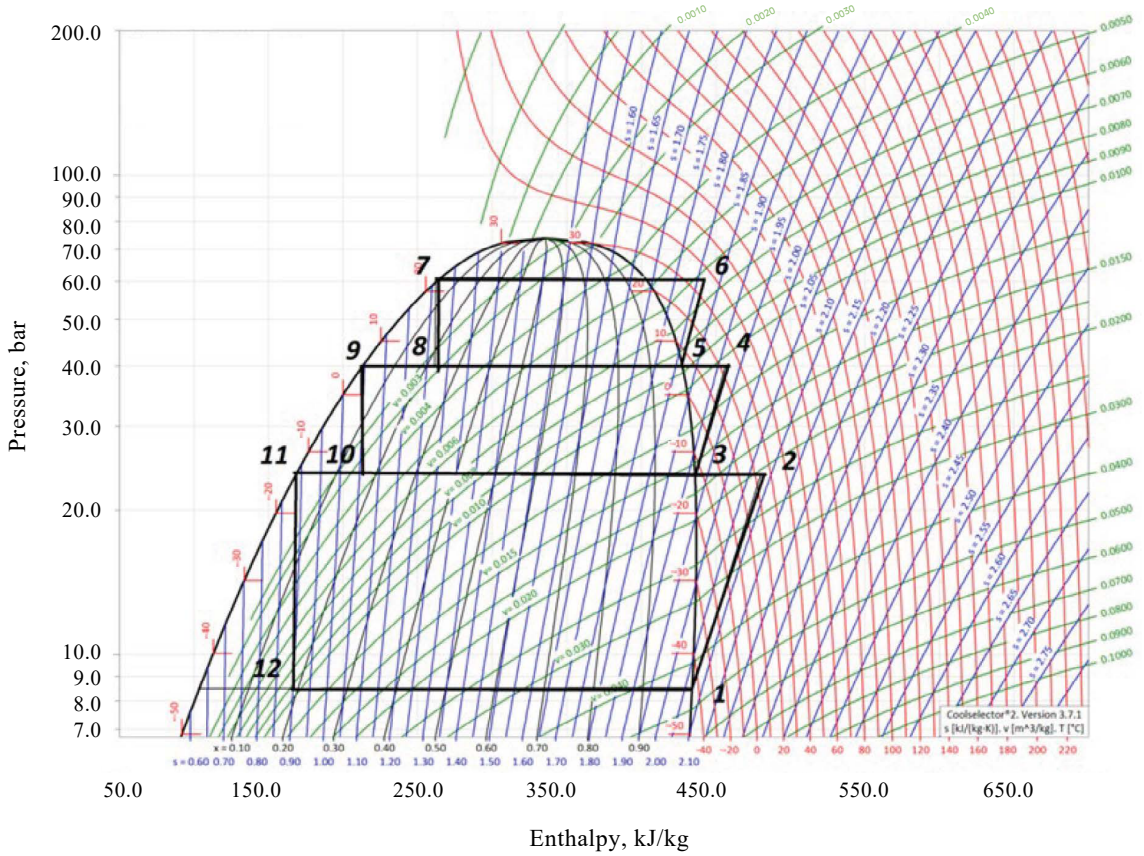


Figure 4 Three-stage CO_2-operating refrigerator: Operating cycle

Table 2 Refrigerant: Nodal parameters

P, MPa	h, kJ/kg	t, °C	V, m³
0.85	440	–50	0.045
2.57	480	25	0.021
2.57	440	–15	0.016
4.28	460	25	0.011
4.28	425	5	0.0085
6.00	445	35	0.0062
6.00	260	22	–
4.28	260	5	–
4.28	210	5	–
2.57	210	–15	–
2.57	170	–15	–
0.85	170	–50	–

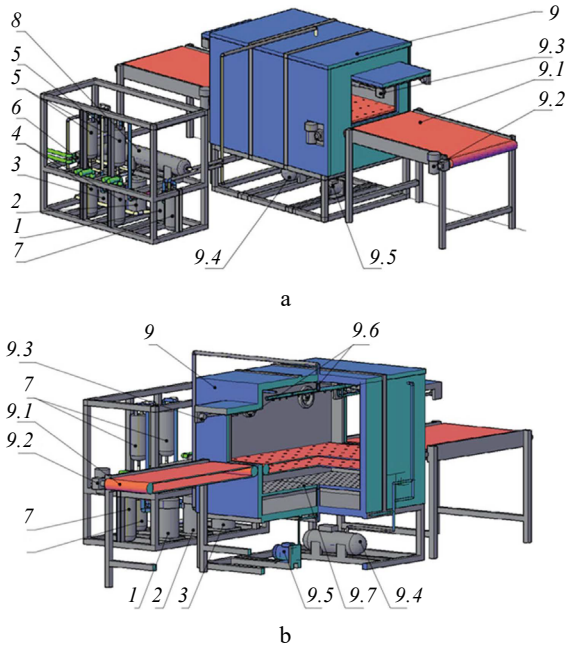


Figure 5 Three-stage CO_2-operating refrigerating unit: 3D model (a) and chamber in section (b)

nozzles. CO_2 snow settles on the product and on the bottom of the chamber. The duct fans (*9.6*) speed up the heat exchange by creating artificial air circulation. As the air passes through the fans, it enters the side cavity of the chamber, moves on to the lower cavity, and passes through the perforated tray (*9.7*). After cooling, CO_2 snow sublimates, and the compressor sucks it out with the help of the liquid separator. The air compressor starts, and the pneumatic pushers open the chamber doors.

We studied the freezing process of turkey carcasses under two conditions: with enforced convection at 3–5 m/s and without it. The experiment involved three cooling temperature modes: –30, –50, and –70°C. When the temperature dropped from –30 to –70°C, the freezing time decreased from 48 to 33 min. When forced convection was applied, it went down to 29 min. Without convection, the mass of CO_2 consumed increased from 7.5 to 13.5 kg; with convection, it rose from 6.5 to 12.0 kg.

Figure 6 shows thermograms of the turkey freezing process at –50 ± 2°C without forced convection. At the initial stage, the inner layer of the meat froze quite intensively, but a severe drop in the cooling rate started after 9 min at +10°C. After 21 min, when the temperature reached +3°C, the cooling slightly accelerated. The latter phenomenon was certainly a positive factor, since the product has to overcome the stage of ice formation and large crystals as quickly as possible to maintain its original quality. Moreover, water crystallization triggers the heat release and reduces the cooling rate.

The freezing process had three stages. As the outer and central layers froze, the boundary of the unfrozen areas shifted toward the inner layer, causing water crystallization in it. It took the outer layer 1–15 min to freeze. The central layer froze a little slower, 1–20 min. Water crystallization in the inner layer began after approximately 25 min. The product cooled down to the set temperature from minute 28 to the end of the freezing process.

Figure 7 shows a graph that illustrates the change in the heat flux density through the outer layer of a turkey carcass during cooling at a refrigerant temperature of –50 ± 2°C without forced convection.

Early in the freezing process, both the decrease in temperature and heat flux intensity were quite rapid due to the lack of preliminary cooling. The heat flux decreased moderately after 3 min. As the inner layer reached the target temperature (–12°C, 38 min), the heat rejection intensity became minimal.

The entire freezing process lasted 41 min and required 10 kg of CO_2. After the freezing, the temperature in the three control points was different, namely –21, –13, and –19°C for the outer, inner, and central layers of the turkey carcass, respectively (Fig. 6).

Figure 8 shows thermograms of the turkey meat freezing at –50 ± 2°C of the refrigerant entering the refrigeration chamber, with forced convection of 3–5 m/s. As expected, the forced convection accelerated the freezing process of the turkey carcass. The entire freezing process lasted 35 min.

The entire freezing process consisted of three stages: cooling to the cryoscopic temperature, freezing, and bringing the product to the targeted temperature. These stages are most clearly observed on the graph of temperature vs. time for the outer layer, where the temperature was the quickest to reach the cryoscopic temperature.

At the initial stage, the outer layer froze quite intensively, but the cooling rate dropped down after 10 min at 0°C, as seen from the flat area in Fig. 8. This process is associated with the early transition of water into ice, which reduces the latent heat. The duration of the phase transition in the outer layer depends on the heat rejection rate and the thickness of the product. In our case, crystallization continued for about 21 min, after which the cooling rate went up slightly.

During the freezing of the outer layer, the boundary of unfrozen areas shifted toward the central layer. As heat rejection from the central layer became more intensive, its temperature approached the cryoscopic value, and crystal formation started in the central part. The freezing process in the inner layer was quite intensive for 17 min, when the cooling rate slowed down due to the cryoscopic temperature.

The central layer froze similarly to the outer one because both were in direct contact with the circulating refrigerant.

After the freezing process was complete, we again detected non-uniformity of the temperature field. The tempe-

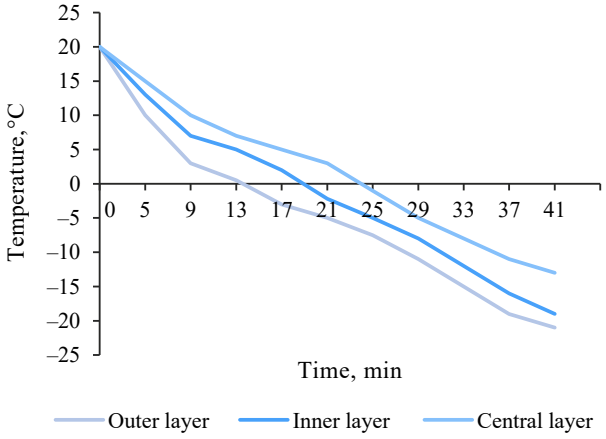


Figure 6 Freezing turkey meat at –50 ± 2°C

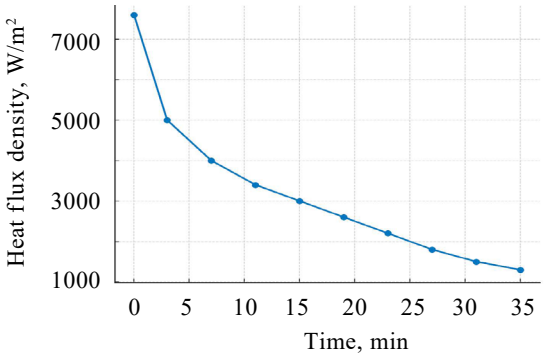


Figure 7 Heat flux density during freezing of turkey carcass with CO_2 at –50 ± 2°C

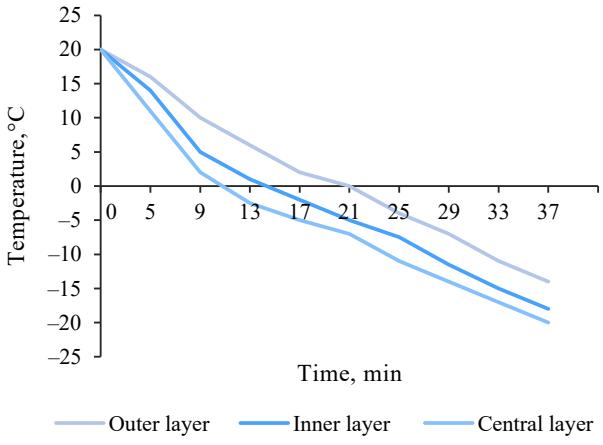


Figure 8 Freezing process of turkey meat at –50 ± 2°C and enforced convection speed of 3–5 m/s

rature values for the outer, inner, and central layers were –18, –12, and –16°C, respectively.

Figure 9 shows the change in heat flux density at –50 ± 2°C of the refrigerant entering the chamber, with an enforced convection rate of 3–5 m/s.

The heat flux density peaked, as expected, at the very onset of cooling when the temperature difference between the turkey carcass and the refrigerant was at its maximum, and the heat rejection process was intensive. The peak value was slightly higher compared to that recorded during the previous experiment, when the temperature was the same but with enforced CO_2 convection.

We used the experimental data on the heat flux density in the Newton-Richman formula to calculate the heat transfer coefficient. The highest value of the heat transfer coefficient was a_{max} = 109 W/(m²·K).

The correlation between the heat transfer coefficient and the time allowed us to conclude that the freezing of the outer layer coincided in time with the cooling of the central layer. The heat flow and the temperature decrease were quite intensive during this stage since the product had not gone through preliminary cooling, and the difference in temperature between the product and CO_2 was maximal. At the next stage, we also observed a moderate decrease in the heat flux level. The cooling of the central layer was almost complete, and the frozen outer layer spread in depth while freezing further. At the final stage, the heat rejection rate was the least intensive since the product continued to freeze down to a given temperature.

The freezing time for a turkey carcass at –30 ± 2°C (without convection) was almost the same as in the experiment with enforced CO_2 convection. Probably, the change in the amount of heat rejected under enforced convection conditions was not very significant compared to the heat of the water crystallization rejected during the freezing of the turkey carcasses.

The freezing lasted 48 min, with 7.5 kg CO_2 consumed. The lowest temperature (–20°C) was recorded in the outer layer at the end of the freezing. The temperature of the inner layer reached –13°C, which corresponded to the target temperature. The temperature in the central part of the turkey carcass was –19°C.

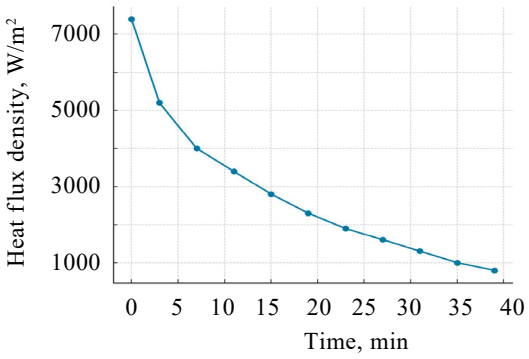


Figure 9 Heat flux density during freezing of turkey carcass with CO_2 at –50 ± 2°C and air convection rate of 3–5 m/s

In the enforced convection experiment, the complete freezing at –30 ± 2°C lasted 43 min, and the amount of carbon dioxide consumed was 6.5 kg. At the end of the freezing process, the lowest temperature in the outer layer was –20°C, i.e., the same as in the experiment without convection, but it was reached by 5 min faster. The inner and central layers also needed 5 min less to reach the temperatures recorded during the experiment without convection (–13 and –19°C, respectively).

Table 3 demonstrates the change in meat temperatures in different layers of the turkey carcass during refrigeration at different refrigerant temperatures, with and without enforced convection. It also presents data on CO_2 consumption required to achieve the target temperature in the inner layer.

In all cases, the freezing of the outer and central layers proceeded quite intensively since these layers were in direct contact with the refrigerant.

The inner layer froze mainly due to the heat rejection to the outer surfaces. The direct heat rejection through the outer layers had a much smaller effect on the intensity of the heat rejection from the inner layer.

Upon reaching the cryoscopic temperature, the inner layer froze less intensively because free (unbound) water in the intercellular space served as a solvent for mineral substances. As free water froze out, the concentration of salts in the unfrozen intercellular solution increased, shifting the cryoscopic temperature to the region of lower temperatures. In this case, water was freezing out gradually, increasing the concentration of the remaining solution. The central layer froze mainly by heat rejection to the internal cavity of the turkey carcass, which contacted

Table 3 Freezing turkey carcasses under different parameters

Enforced confection	Chamber temperature, °C	Layer	Treatment time, min				CO_2, kg
			30	35	40	50	
			Temperature, °C				
0	–30	outer	–7	–13	–15	–20	7.5
		inner	–3	–7	–9	–13	
		central	–5	–11	–13	–19	
	–50	outer	–11	–19	–21	–	10.0
		inner	–5	–11	–13	–	
		central	–8	–16	–19	–	
	–70	outer	–14	–20	–	–	13.5
		inner	–7	–14	–	–	
		central	–11.5	–18.0	–	–	
3–5	–30	outer	–10	–16	–18	–	6.5
		inner	–4	–9	–11	–	
		central	–7.5	–13.5	–16.5	–	
	–50	outer	–12	–18	–	–	9.0
		inner	–6	–12	–	–	
		central	–10	–16	–	–	
	–70	outer	–16	–	–	–	12.0
		inner	–10	–	–	–	
		central	–14	–	–	–	

with CO_2. After most unbound water crystallized, the temperature decrease accelerated again.

At the end of freezing, the temperature was different at different sensor points, i.e., the temperature field was uneven. The crystal formation directly depended on the freezing rate, which, in its turn, depended on the rate at which the interface moved between the liquid and solid phases from the surface of the frozen product to its thermal center.

At –70 ± 2°C, the process was very similar to the those described for –30 and –50°C, but it occurred much faster. The curves of the temperature fields showed that the freezing process without enforced convection was less intense and lasted 33 min. Enforced convection of the refrigerant at the fan outlet reduced the freezing time to 29 min. The CO_2 consumption was 13.5 and 12.0 kg, respectively, with or without enforced convection.

At a chamber temperature of –70°C and intensive convection, the preliminary cooling with CO_2 snow and temperature unification occurred most quickly. The preliminary cooling eliminated subsequent cracking of the carcass and, therefore, reduced weight loss associated with defrosting and cooking.

In the surface layer, crystals formed quite fast in all experiments due to its thinness and direct contact with CO_2. As crystallization started in the central layer, it prevented the rest of the product from supercooling since the linear speed of crystallization almost always exceeded the heat rejection rate, causing exchange diffusion between the layers. As the heat transfer coefficient changed, water moved from the inner, unfrozen layer to the outer, frozen one. Conversely, the freezing process made dissolved substances move from the outer layer to the inner one. Maximal freezing intensity was required to preserve moisture: if the heat rejection rate was insufficient, the inward movement of the frozen layer boundary was less than the exchange diffusion rate. A significant portion of the moisture began to move towards the surface of the product, freezing the moisture out of the product.

CONCLUSIONS

We developed a three-stage R744-operating refrigeration unit using heat inflow calculations and a careful selection of primary and auxiliary equipment. Based on direct contact of CO_2 with the product, the unit demonstrated an admirable economic efficiency, as well as prospects for automating the freezing of turkey carcasses. The refrigeration chamber was enlarged and provided with a conveyor belt and automatic doors. The CO_2 recirculation also added to its economic efficiency and compliance with environmental requirements.

The unit owed its high efficiency to direct contact of CO_2 snow and gas with frozen turkey. The enforced convection in the chamber made it possible to reduce the freezing time and ensure the uniformity of cooling, which helped preserve the quality of the product. CO_2 snow and gas allowed us to minimize mechanical damage to the meat structure, which often accompanies traditional freezing methods.

The automation system included pneumatic pushers and a vacuum pump, which boosted the productivity and reduced labor costs. The chamber performed well at various temperatures and air-gas flux rates, which makes the refrigerator a universal solution for all kinds of food industry enterprises.

To improve the freezing process, the phase changes of water in meat should be taken into account, with an outlook for the shortest phase transition time.

The study contributes to the evolution of food freezing. In addition to turkey meat, the new three-stage R744-operating refrigeration unit may be applied to a wide range of commercial foods. Further research will improve the efficiency and quality of the freezing process.

CONTRIBUTION

E.N. Neverov supervised the project; P.S. Korotkih collected, analyzed, and also interpretated the data; A.K. Gorelkina developed the experimental refrigerating chamber and conducted the experiments; I.V. Timoshchuk wrote the manuscript.

CONFLICT OF INTEREST

The authors declared no potential conflict of interest regarding the research, authorship, and/or publication of this article.

REFERENCES

1. Kálmán Á, Szőllősi L. Global Tendencies in turkey meat production, trade and consumption. Acta Agraria Debreceniensis. 2023;(2):83–89. https://doi.org/10.34101/actaagrar/2/12594
2. Zimnyakov VM, Varlamova YeN. The state and prospects of turkey meat production. Niva Povolzhya. 2017;(4): 55–62. (In Russ.) https://elibrary.ru/ZTIEKD
3. Askerov PF, Rabadanov AR, Kibirov KG, Tolparov EB, Bondarenko OV, *et al*. Role and importance of turkey meat production in poultry farming in Russia: Prospects for further development. Entomology and Applied Science Letters. 2021;8(3):15–20. https://doi.org/10.51847/IE9jQz8ugz
4. Nastasevich I, Lakitsevich B, Petrovich Z. Cold chain management in meat supplies: Old vs. new strategies. Theory and Practice of Meat Processing. 2017;2(4):20–34. (In Russ.) https://doi.org/10.21323/2414-438X-2017-2-4-20-34
5. Meretukova FN, Abregova NV. Quality indicators of semi-finished sous-vide products from turkey meat. New Technologies. 2021;17(2):48–55. (In Russ.) https://doi.org/10.47370/2072-0920-2021-17-2-48-55

6. Shakhnazarova LV, Stefanova IL, Klimenkova AYu. Use of turkey meat for the production of specialized food. Bird and poultry products. 2022;(4):64–68. (In Russ.) https://doi.org/10.30975/2073-4999-2022-24-4-64-68
7. Solaesa AG, García-Barroso C, Romero C, González C, Jiménez P, *et al*. Nutritional composition and technological properties determining the quality of different cuts of organic and conventional Turkey meat. Poultry Science. 2024;103(12):104331. https://doi.org/10.1016/j.psj.2024.104331
8. Russian turkey farming: confident growth continues. Scientific and practical journal for managers and specialists of the agro-industrial complex. [cited 2025 Apr 30] (In Russ.) Available from: https://zzr.ru/zzr-2025-03-001
9. Ishevsky AL, Davydov IA. Freezing as a method of food preservation. Theory and Practice of Meat Processing. 2017;2(2):43–59. https://doi.org/10.21323/2414-438X-2017-2-2-43-59
10. Anisimova KV, Protopopova KA, Spiridonov AB, Ipatova AF, Stepanova TO. Development of a laboratory installation for freezing meat, fish and fruit. AgroEcoInfo. 2023;(1):34. (In Russ.) https://elibrary.ru/XZTIYG
11. Ikram A, Arshad MT, Maqsood S, Safdar SZ, Rasheed A, *et al*. Modern approaches for ensuring the safety and integrity of frozen foods: An overview. Food and Agricultural Immunology. 2025;36(1):2491594. https://doi.org/10.1080/09540105.2025.2491594
12. Dang DS, Bastarrachea LJ, Martini S, Matarneh SK. Crystallization behavior and quality of frozen meat. Foods. 2021;10(11):2707. https://doi.org/10.3390/foods10112707
13. Young-Chan Y, Honggyun K, Karna R, Geun-Pyo H. Evaluation of the relationship between freezing rate and quality characteristics to establish a new standard for the rapid freezing of pork. Food Science of Animal Resources. 2021;41(6):1012–1021. https://doi.org/10.5851/kosfa.2021.e52
14. Maina P, Huan Z. A review of carbon dioxide as a refrigerant in refrigeration technology. South African Journal of Science. 2015;111(9/10):10. https://doi.org/10.17159/sajs.2015/20140258
15. Barta RB, Groll EA, Ziviani D. Review of stationary and transport CO_2 refrigeration and air conditioning technologies. Applied Thermal Engineering. 2021;185:116422. https://doi.org/10.1016/j.applthermaleng.2020.116422
16. Boupda O, Tessemo H, Fongang I, Nyami F, Lontsi F, *et al*. A review on technologies for the use of CO_2 as a working fluid in refrigeration and power cycles. Energy and Power Engineering. 2024;16(6):217–256. https://doi.org/10.4236/epe.2024.166011
17. Loktionov DG. Auto-refrigeration units on carbon dioxide. Scientific and Technical Support of Refrigeration Industry: Conf. proceedings. All-Russian Research Institute of Refrigeration Industry. Moscow, 2010;92–95. (In Russ.). https://elibrary.ru/RSDWYP
18. Shao L-L, Zhang C-L. Thermodynamic transition from subcritical to transcritical CO_2 cycle. International Journal of Refrigeration. 2016;64:123–129. https://doi.org/10.1016/j.ijrefrig.2016.01.018
19. Sharma DK, Hazarika MM, Ramgopal M. The optimum discharge pressure of CO_2-based refrigeration cycles operating under subcritical and transcritical conditions. International Journal of Ambient Energy. 2023;44(1):1232–1242. https://doi.org/10.1080/01430750.2023.2171483
20. Neverov EN, Korotky IA, Plotnikov IB, Korotkiy PS, Kozhaev AA. The study of the parameters of the heat transfer process at carbon dioxide sublimation. Bulletin of KSAU. 2020;(6):215–222. (In Russ.) https://doi.org/10.36718/1819-4036-2020-6-215-222
21. Ji H, Pei J, Cai J, Ding C, Guo F, *et al*. Review of recent advances in transcritical CO_2 heat pump and refrigeration cycles and their development in the vehicle field. Energies. 2023;16(10):4011. https://doi.org/10.3390/en16104011
22. Burak LCh. Prospects for the use of supercritical carbon dioxide technology in the food industry. Subject field overview. Polzunovskiy vestnik. 2025;(1):32–50. (In Russ.) https://doi.org/10.25712/ASTU.2072-8921.2025.01.004
23. Tosato G, Minetto S, Rossetti A, Hafner A, Schlemminger C, *et al*. Field data of CO_2 integrated refrigeration, heating, and cooling systems for supermarkets. Proceedings of the 14th IIR-Gustav Lorentzen Conf. on Natural Refrigerants. Kyoto, 2020:1162. https://doi.org/10.18462/iir.gl.2020.1162
24. Panão MRO, Franco PAG, Costa JJ. Effect of atomizer geometry on particle formation in dry-ice sprays. International Journal of Multiphase Flow. 2020;130:103358. https://doi.org/10.1016/j.ijmultiphaseflow.2020.103358

ORCID IDs
Evgeniy N. Neverov https://orcid.org/0000-0002-3542-786X
Pavel S. Korotkih https://orcid.org/0000-0002-4546-0276
Alena K. Gorelkina https://orcid.org/0000-0002-3782-2521
Irina V. Timoshchuk https://orcid.org/0000-0002-1349-2812